Relative Magnitudes of the Short-Term Motions of the Cyclic and Linear Components of a Homopolyrotaxane in Θ Media

Sagar S. Rane and Wayne L. Mattice*

Maurice Morton Institute of Polymer Science, The University of Akron, Akron, Ohio 44325-3909

Received April 29, 2004; Revised Manuscript Received June 21, 2004

ABSTRACT: The motions of a homopolyrotaxane composed of polyoxyethylene have been studied at 373 K in the dense melt and in systems obtained by dilution with a structureless Θ solvent. The sizes of the rings vary from $(CH_2CH_2O)_{10}$ to $(CH_2CH_2O)_{20}$. The dynamic Monte Carlo simulation employs a coarse-grained representation of the system that is constrained so that an atomistically detailed description can be obtained from any replica. Single bead moves, corresponding to the motion of 2−3 backbone atoms in the atomistically detailed model, are employed in the study of the dynamics. The motion has the characteristics of a one-dimensional random walk when it is monitored by recording the index of the bead in the linear chain that is the instantaneous site of the threading of the cyclic component. When the same simulation is monitored in a laboratory coordinate system, the motions in the systems with the structureless diluent are dominated by subchains of the linear chain component of the homopolyrotaxane, with only a minor contribution from the motion of the ring. In the dense melts the motions of the linear chain and the ring can be more similar in size, but no circumstances were found under which the motion of the ring became dominant over the motion of the linear component.

Introduction

The concept of topological isomerism, which includes structures such as rotaxanes and catenanes, was introduced over four decades ago.[1,2] The simplest rotaxane consists of a linear molecule that is threaded by a single macrocyclic ring. This structure becomes a catenane if the two ends of the linear component are linked by a covalent bond. The two components of the catenane cannot be dissociated without the rupture of covalent bonds, in contrast with the rotaxane, where the macrocyclic component might slip off the linear chain unless that process is prevented by the introduction of bulky end groups. The term pseudorotaxane identifies a rotaxane that does not have end groups that act as stoppers to prevent dethreading.

Although the separated components can have different translational diffusion coefficients, D, both components in the catenane or the rotaxane with stoppers must have the same value of D because, in absence of dissociation, the mean-square displacement of their centers of mass approach the same value in the limit as $t \rightarrow \infty$.[3] This requirement does not, however, imply that the short-term motions of the two components of the homopolyrotaxane must be similar.

In rotaxanes, there is ample evidence for a process often termed shuttling, where the cyclic component shifts from one position to another along the linear chain.[4−10] Computational studies of this process may evaluate the energy of the system as the macrocyclic component is translated along the linear component.[5] This computation can reveal the locations and spacings of energy minima along this "reaction coordinate" and also identify the heights of the barriers that separate energy minima or translational isomers.[10] This information can lead to estimates of a hopping rate and the distance traversed in each hop. These calculations may be performed in a nonviscous environment that might be as simple as a vacuum.

This type of characterization of the short-term internal motions of the rotaxane is indeed important, but potential applications require that this information be supplemented by another description of the short-term motions. For example, if a rotaxane were envisioned as a component of a nanodevice, there would be interest in the characterization of the motions in a laboratory coordinate system, where the shuttling process must lie somewhere between two limiting types of behavior. At one limit is the shuttling of a mobile macrocyclic component along a static linear chain, and at the other limit is the slithering of a mobile linear chain through the constraint imposed by a static macrocyclic ring. These two extremes are suggested in cartoon form in Figure 1. We now seek from simulation a description of accessible possibilities within this continuum of potential behavior; when the two components of the rotaxane are constructed from the same monomer unit, the macrocycle is kept small enough so that spontaneous and simultaneous threading by two linear chains is unlikely, the environment supports the unperturbed (Θ) state of the polymer, and the viscosity of this Θ medium

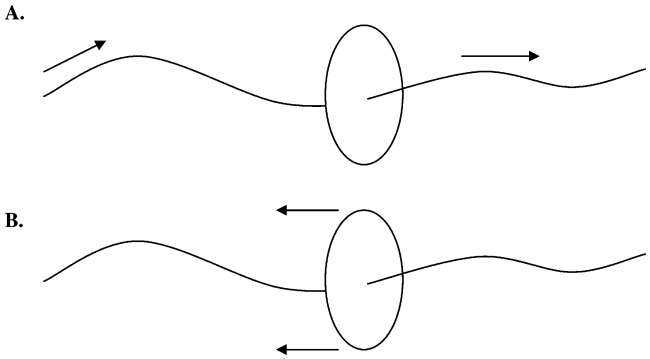

Figure 1. A cartoon that depicts the two extreme possibilities for the short-term motion of the components of a rotaxane, as viewed in a laboratory coordinate system. Part A shows the slithering of the linear chain through a static ring, and part B shows the shuttling of a ring along a static linear chain. These two extremes are not distinguishable in a record of the time dependence of the position of the ring along the linear chain.

10.1021/ma049159c CCC: $27.50
Published on Web 08/07/2004

varies from nil up to the viscosity of the polymer melt. The simulation readily finds conditions where the dominant spontaneous short-term motion in the laboratory coordinate system is provided by the linear subchain. The simulation never finds conditions where the dominant short-term motion arises from the ring component.

The same monomer unit, OCH_2CH_2, is chosen for both components in this study. Although the synthesis is difficult, homopolyrotaxanes of polyoxyethylene have been prepared recently.[11] Homopolyrotaxanes are especially attractive for present purposes because the monomer units in the linear and cyclic species must have the same intrinsic mobility because they are exactly the same species. Any differences in the dynamics of the two components of the homopolyrotaxane must therefore arise from the inherent differences in the mobility of a linear and cyclic component in this environment.

We exploit a recently developed bridging method[12] for the reversible interconversion of coarse-grained and atomistically detailed descriptions of a polyoxyethylene melt.[13] Previous Monte Carlo (MC) simulations of the static properties of this system allowed the detection and characterization of the extent of spontaneous threading in a two-component melt composed of linear and cyclic species of polyoxyethylene, either in the melt[13] or in a Θ solvent.[14] Here we use a dynamic MC simulation to characterize the relationship between the mobility of the macrocyclic component and the linear subchain, as monitored in a laboratory coordinate system.

Simulation Method and Details

The simulations are performed on a high-coordination lattice, with $10i^2 + 2$ cells in shell i, that has been used previously in simulations of polyethylene,[15] polypropylene,[16] poly(vinyl chloride),[17] and polystyrene[18] as well as polyoxyethylene.[13,14] Jernigan has also used this high-coordination lattice for the simulation of globular proteins.[19] One coarse-grained bead is assigned to every second atom in polyoxyethylene, so that the number of monomer units in a ring is $^2/_3$ of the number of beads used in its coarse-grained representation. The step length on the high-coordination lattice is obtained from the lengths of the C−C and C−O bonds, l_{CC} and l_{CO}, as $[(8/9)(l_{CC}^2 + 2l_{CO}^2)]^{1/2} = 2.39$ Å. The simulations were performed in a three-dimensional box with an angle of 60° between any two axes. Periodic boundary conditions were employed in all directions. Each side of the box has 20 steps on the high-coordination lattice, corresponding to a distance of 47.8 Å. The density of a polyoxyethylene melt at 373 K, the temperature of the simulation, is obtained with occupancy of 21% of the sites on the high-coordination lattice.

During the simulation, two types of constraints are employed to force the coarse-grained chains to mimic polyoxyethylene. A short-range intramolecular constraint is devised by mapping a rotational isomeric state model for polyoxyethylene[20] onto the coarse-grained description of the chain. This mapping enforces the proper distribution of trans and gauche states at C−C and C−O bonds and properly incorporates the short-range intramolecular effects of the electrostatic interactions of the dipole in successive ether units.[13] Longer range intramolecular interactions, and all intermolecular interactions, are obtained using a discretized version of a continuous, spherically symmetric Lennard-Jones potential energy function with $\epsilon/k_B = 154$ K and $\sigma = 3.76$ Å.[13] The discretization, via the averaged Mayer f-function, is performed in a manner that enforces the same value of the second virial coefficient from the derived discrete function and its continuous parent.[21] At the temperature of the simulation, the first three shells have energies of 8.113, −0.213, and −0.339 kJ/mol. Higher shells, which all have negative energies that are much weaker than −0.339 kJ/mol, are ignored in the simulation. This discretized Lennard-Jones potential has been demonstrated to produce the correct density for bulk polyoxyethylene at this temperature, in a simulation where the system is free to find its own density.[13]

The dynamic MC simulations are performed using single beads moves only.[15] Each single bead move corresponds to a local displacement of two or three backbone atoms in the atomistically detailed description of the system.[15] A Monte Carlo step (MCS) is that portion of the simulation where there is one attempt, on average, to move each bead in the system. Moves that would produce double occupancy of a site or collapses are rigorously disallowed. A collapse occurs in configurations of two successive coarse-grained bonds that avoid double occupancy of the high-coordination lattice but produce double occupancy on the underlying diamond lattice when all atoms are restored to the detailed description of the system.[15] If a proposed move produces neither double occupancy nor collapse, its acceptance is determined by the usual Metropolis criteria.[22] Intramolecular pivot moves of 2−6 beads[23] were employed during preequilibration of the models, before initiation of the dynamic MC runs, but these pivot moves were excluded from the actual dynamic MC runs. Preequilibration typically used 5 million MCS, after which an additional 1 million MCS was used for the dynamic MC simulation. These runs are well in excess of the times required for the decay to zero of the autocorrelation function defined by the end-to-end vector, $\langle \mathbf{r}(t+t_0)\cdot\mathbf{r}(t_0)\rangle$, for the linear subchains of interest. They are also longer than the times required for these subchains and the rings to experience mean-square displacements of their centers of mass that exceed their squared radii of gyration.

Threading events were characterized by the procedure described in detail by Helfer et al.[13] This analysis used atomistically detailed representations of the system that were generated by restoring the missing chain atoms to a coarse-grained replica of the system.[15]

The sizes of the components in the simulation exploit a limiting condition that blurs the distinction between a rotaxane and a catenane. In real rotaxanes of finite size, bulky stoppers are used to prevent dethreading. Conceptually, dethreading of a rotaxane is also suppressed by taking the limit of infinite degree of polymerization for the linear component. In this limit, the macrocyclic component of finite size will never find an end of the linear component. If the macrocyclic component cannot find the ends of the linear component, its behavior is not affected by covalently linking these ends to form a catenane. Therefore, similar behavior must be seen in the short-term motion of a small macrocyclic component on a very long linear chain in a rotaxane and for the same macrocyclic component when combined with a much larger ring to make a catenane. Although we will interpret the results of our simulation as being

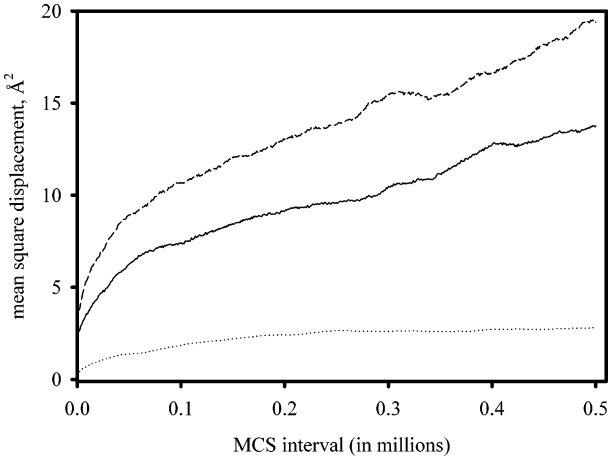

Figure 2. Mean-square displacements $g_d(t)$ (dashed line), $g_b(t)$ (solid line), and $g_r(t)$ (dotted line), reading from top to bottom on the figure, when the ring is coarse-grained $(CH_2CH_2O)_{14}$ and the system is at bulk density at 373 K.

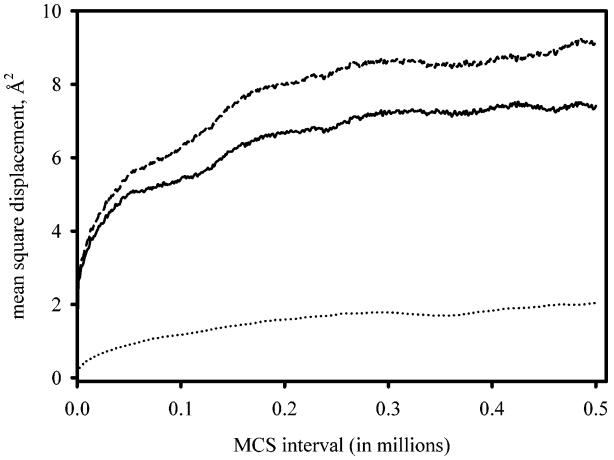

Figure 3. Mean-square displacements $g_d(t)$ (dashed line), $g_b(t)$ (solid line), and $g_r(t)$ (dotted line), reading from top to bottom, when the ring is coarse-grained $(CH_2CH_2O)_{20}$ and the system is at bulk density at 373 K.

relevant to rotaxanes, most of the simulations actually study catenanes in which the two components are of drastically different sizes. This choice of topological isomers has the advantange that we eliminate the possibility of dethreading during the simulation. Specifically, the system contains equal numbers of rings represented by N_r and $330 - N_r$ beads, with N_r in the range 15−30. All of these rings appear as catenanes, with each catenane composed of one small and one large ring. Henceforth, we will equate the small and large components of the catenane to the cyclic and linear components of a rotaxane for the purpose of the analysis of their short-term motions in a laboratory coordinate system.

The introduction of the Θ solvent was achieved by erasing $^4/_5$ of the catenanes in the simulation of the melt at a density of 1.06 g/cm^3. If the simulation is continued, but with a revised intermolecular potential obtained by multiplying the second and third shell energies for the original discretized Lennard-Jones potential by a factor of 0.63, there is almost no difference in the mean-square dimensions of the linear chain in a dense melt and in the diluted system.[13] The near equivalence of these dimensions in the dense melt and in less dense system obtained by erasing some of the chains shows that the diluent acts as a structureless, implicit Θ solvent for the polymer. Since this implicit Θ solvent is structureless, its viscosity is nil.

Mobilities for Systems in the Dense Melt

Figure 2 depicts mean-square displacements for the system where the smaller component is represented by 21 coarse-grained beads, corresponding to the ring with composition $(CH_2CH_2O)_{14}$. The larger component is represented by 309 coarse-grained beads. The equimolar mixture is present at the density of 1.06 g/cm^3, corresponding to the density expected for a polyoxyethylene melt at the temperature of the simulation, 373 K.[24] The two components occur in pairs, with one of the smaller rings threaded onto each molecule of the larger component. The mean-square displacement of the center of mass of the ring represented by 21 coarse-grained beads is depicted by the dotted line near the bottom of Figure 2. This displacement, denoted by $g_r(t)$, is calculated from the time-dependent vector, denoted by $\mathbf{R}_r(t)$, that points to the location of the center of mass of the ring in a laboratory coordinate system.

$$g_r(t) = \langle[\mathbf{R}_r(t + t_0) - \mathbf{R}_r(t_0)]\cdot[\mathbf{R}_r(t + t_0) - \mathbf{R}_r(t_0)]\rangle \quad (1)$$

Angle brackets denote the average over all rings and over all time origins, t_0. The solid line in the same figure denotes the mean-square displacement of the bead in the larger component that was the site at which the smaller component was threaded at t_0. This displacement, $g_b(t)$, is calculated from the vector that points to the designated bead, $\mathbf{R}_b(t)$.

$$g_b(t) = \langle[\mathbf{R}_b(t + t_0) - \mathbf{R}_b(t_0)]\cdot[\mathbf{R}_b(t + t_0) - \mathbf{R}_b(t_0)]\rangle \quad (2)$$

These two displacements must become indistinguishable in the limit as $t \rightarrow \infty$ because the small ring cannot escape from its larger partner. Since the translational diffusion coefficient, D, is defined in this limit, both species have the same value of D. This limit, which is not easily obtainable in our simulation, is not relevant for present purposes. Instead, interest is confined to the earlier part of the simulation, where the two types of displacements might be different, as indeed they are. At short times, that portion of the linear chain that was the initial site of threading has greater mobility that does the ring. This qualitative conclusion applies also when the size of the ring is increased to 30 beads, corresponding to $(CH_2CH_2O)_{20}$, as shown in Figure 3.

The third, and topmost, curve in Figures 2 and 3 measures the evolution with time of the mean-square difference in the location of the reference bead on the linear chain and the center of mass of the ring. It is calculated as shown in eq 3.

$$g_d(t) = \langle[\mathbf{R}_b(t + t_0) - \mathbf{R}_b(t_0) - \mathbf{R}_r(t + t_0) + \mathbf{R}_r(t_0)]\cdot[\mathbf{R}_b(t + t_0) - \mathbf{R}_b(t_0) - \mathbf{R}_r(t + t_0) + \mathbf{R}_r(t_0)]\rangle \quad (3)$$

If the ring and reference bead in the linear chain were moving in the same direction, but at different velocities, such that $g_b(t) > g_r(t)$, as shown in Figures 2 and 3, we would expect to find $g_b(t) > g_d(t) > g_r(t)$. Instead, the simulation finds $g_d(t) > g_b(t) > g_r(t)$. This result requires that the ring and reference bead are not always moving in the same direction. Such a result is consistent with the ring giving the appearance of a random walk along the linear chain, when the mobility is monitored locally

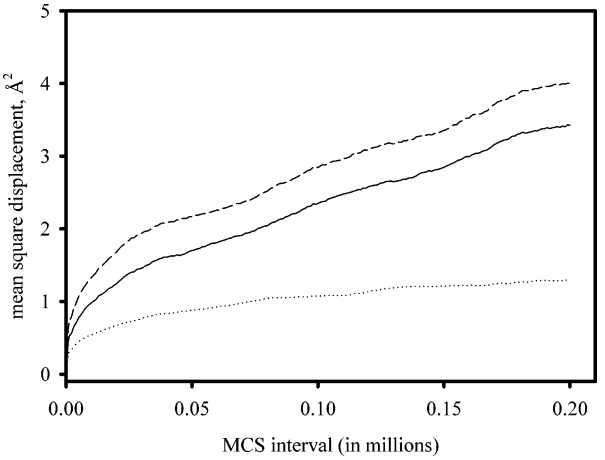

Figure 4. Mean-square displacements $g_{d'}(t)$ (dashed line), $g_s(t)$ (solid line), and $g_r(t)$ (dotted line), reading from top to bottom, when the ring is coarse-grained $(CH_2CH_2O)_{10}$ and the system is at bulk density at 373 K.

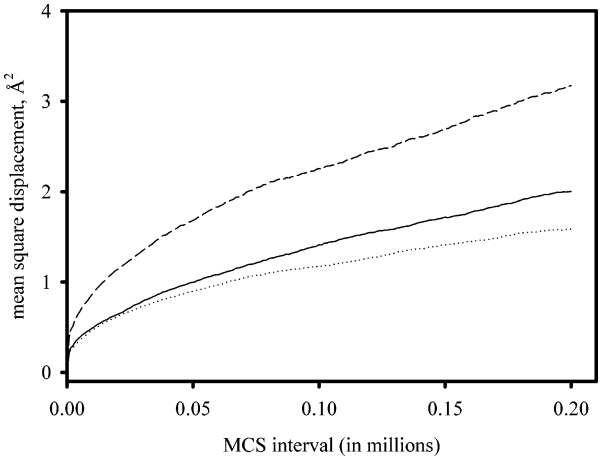

Figure 5. Mean-square displacements $g_{d'}(t)$ (dashed line), $g_s(t)$ (solid line), and $g_r(t)$ (dotted line), reading from top to bottom, when the ring is coarse-grained $(CH_2CH_2O)_{20}$ and the system is at bulk density at 373 K.

by simply recording the time dependence of the position on the linear chain to which the ring is threaded. A separate analysis of the motions, not described here, confirms that the motion sensed in this local coordinate system does indeed have the characteristics of a random walk in the simulation.

Before drawing conclusions from simulations reported in Figures 2 and 3, attention needs to be given to the fact that $g_b(t)$ measures the mobility of a single bead, but $g_r(t)$ measures the mobility of the center of mass of a collection of beads. This difference alone is likely to contribute to the finding that $g_b(t) > g_r(t)$. To remove this factor from the comparison, we also calculate the mean-square displacement of the center of mass of a subchain of the larger component. This subchain has the same number of beads as the ring, and its central bead is the one to which the ring was threaded at zero time. Let $\mathbf{R}_s(t)$ be the vector in the laboratory coordinate system that points to the center of mass of this subchain at time t.

$$g_s(t) = \langle[\mathbf{R}_s(t + t_0) - \mathbf{R}_s(t_0)]\cdot[\mathbf{R}_s(t + t_0) - \mathbf{R}_s(t_0)]\rangle \quad (4)$$

Also define a counterpart of $g_d(t)$ as shown in eq 5, using $\mathbf{R}_s(t)$ in place of $\mathbf{R}_b(t)$.

$$g_{d'}(t) = \langle[\mathbf{R}_s(t + t_0) - \mathbf{R}_s(t_0) - \mathbf{R}_r(t + t_0) + \mathbf{R}_r(t_0)]\cdot[\mathbf{R}_s(t + t_0) - \mathbf{R}_s(t_0) - \mathbf{R}_r(t + t_0) + \mathbf{R}_r(t_0)]\rangle \quad (5)$$

The time evolutions of $g_r(t)$, $g_s(t)$, and $g_{d'}(t)$ are depicted in Figures 4 and 5 for systems where the ring is coarse-grained $(CH_2CH_2O)_{10}$ and $(CH_2CH_2O)_{20}$, respectively. For the smaller ring, the behavior is qualitatively similar to that depicted in Figures 2 and 3, with $g_{d'}(t) > g_s(t) > g_r(t)$. The small ring undergoes a random walk along the chain, insofar as its position on the chain is concerned, but the main motion in the laboratory coordinate system is not from the ring, but instead from the subchain of the same size in the linear chain. As the ring becomes larger, requiring that the subchain in the linear chain also be made larger, there is a decrease in the difference in the mobilities, as sensed in the laboratory coordinate system, as shown by comparison of Figures 4 and 5. However, the mobility of the ring remains smaller than the mobility of the corresponding linear subchain, $g_s(t) > g_r(t)$.

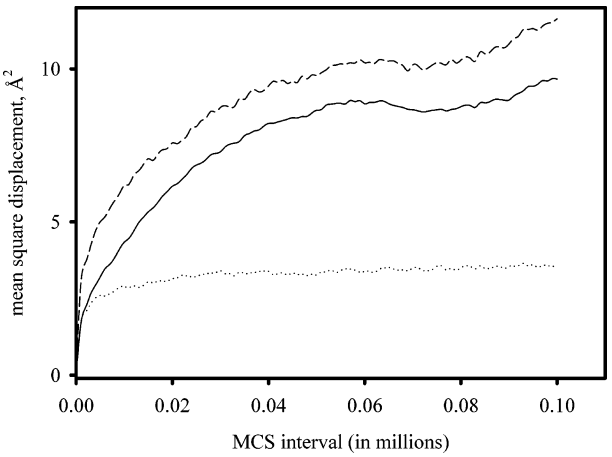

Figure 6. Mean-square displacements $g_{d'}(t)$ (dashed line), $g_s(t)$ (solid line), and $g_r(t)$ (dotted line), reading from top to bottom, when the ring is coarse-grained $(CH_2CH_2O)_{10}$ and the system is in an implicit Φ solvent at 373 K and a concentration of 0.20, expressed as volume fraction polyoxyethylene.

In the dense melt, the small cyclic component of the rotaxane does not have a short-term mobility that exceeds the motion expected for the linear subchain of the same size that was centered at the site of threading at t_0. The short-term motion in the laboratory coordinate system contains a significant contribution from the motion of the linear chain, and in some cases the linear chain may dominate the motion sensed in the laboratory coordinate system. We now inquire whether this qualitative conclusion might require modification if the motions were to take place in a medium that is less viscous than the polymer melt.

Motion in a Θ Solvent

The system used for the study of the motion in a Θ solvent was constructed by removing $^4/_5$ of the large and small components from the system used for the simulation in the dense melt. On this basis, the concentration of polyoxyethylene is 0.20, when expressed as a volume fraction. The shell energies were then modified so that the mean-square dimensions of the linear chain are essentially unchanged, as described by Xu et al.[14] The structureless medium therefore mimics a Θ solvent. Since the medium contains no beads whatsoever, it must be of very low viscosity.

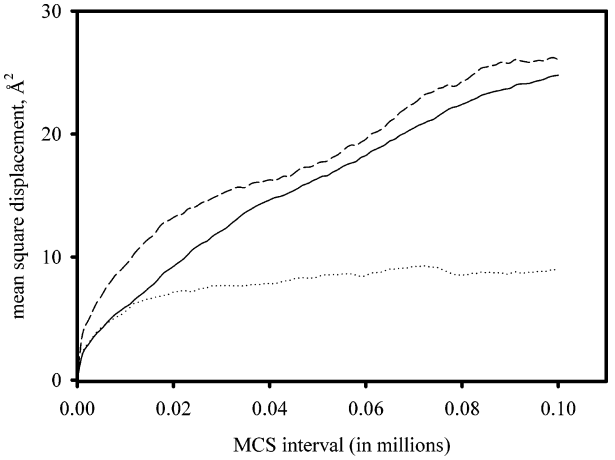

Figure 7. Mean-square displacements $g_{d'}(t)$ (dashed line), $g_s(t)$ (solid line), and $g_r(t)$ (dotted line), reading from top to bottom, when the ring is coarse-grained $(CH_2CH_2O)_{20}$ and the system is in an implicit Φ solvent at 373 K and a concentration of 0.20, expressed as volume fraction polyoxyethylene.

Figures 6 and 7 depict the mobilities of two systems in the Φ solvent, with the analysis being based on $g_{d'}(t)$, $g_s(t)$, and $g_r(t)$. The mobilities of all species are higher in the presence of the diluent than they were in the dense melt, as is apparent upon comparison of Figures 5 and 7, where the ring is a coarse-grained representation of $(CH_2CH_2O)_{20}$. More importantly, the systems with diluent have $g_{d'}(t) > g_s(t) > g_r(t)$, with $g_s(t)$ being much closer to $g_{d'}(t)$ than to $g_r(t)$. In this medium of lower viscosity, the short-term motion sensed in a laboratory coordinate system is dominated by the motion of the linear subchain. The cartoon in part A of Figure 1 is a better representation of this motion than is the cartoon in part B.

Conclusions

The simulations provide no support for the conjecture that the spontaneous short-term motions of a homopolyrotaxane, as sensed in a laboratory coordinate system, are dominated by the shuttling of the ring along a stationary linear chain. In a dense system, such as a melt, there may be circumstances where nearly equivalent contributions to this motion are provided by the ring and by the linear chain. However, when the system is diluted with a low-viscosity Θ solvent, there is a stronger enhancement in the motion of the linear subchain than in the motion of the ring, causing motion of the linear subchain to dominate the short-term dynamics sensed in the laboratory coordinate system.

Since the simulations were performed for a homopolyrotaxane, they do not address the situation in dense melts of polyrotaxanes in which the linear and cyclic components are constructed from different monomer units. Conceivably such systems might produce a different result due to the enthalpic interaction of the two chemically distinguishable types of monomer units or to inherent differences in the mobilities of these monomer units. Since it is unlikely that a single liquid would be a Θ solvent for both components in such cases, the diluent might also produce different behavior than that seen here with the homopolyrotaxane.

Acknowledgment. This research was supported by National Science Foundation Grant DMR 0098321.

References and Notes

(1) Wasserman, E. *J. Am. Chem. Soc.* **1960**, *82*, 4433.
(2) Frisch, H. L.; Wasserman, E. *J. Am. Chem. Soc.* **1961**, *83*, 3789.
(3) Zhao, T.; Beckham, H. W.; Gibson, H. W. *Macromolecules* **2003**, *36*, 4833.
(4) Credi, A.; Balzani, V.; Langford, S. J.; Stoddart, J. F. *J. Am. Chem. Soc.* **1997**, *119*, 2679.
(5) Raymo, F. M.; Houk, K. N.; Stoddart, J. F. *J. Org. Chem.* **1998**, *63*, 6523.
(6) Brouwer, A. M.; Frochot, C.; Gatti, F. G.; Leigh, D. A.; Mottier, L.; Paolucci, F.; Roffia, S.; Wurpel, G. W. H. *Science* **2001**, *291*, 2124.
(7) Asakawa, M.; Brancato, G.; Fanti, M.; Leigh, D. A.; Shimizu, T.; Slawin, A. M. Z.; Wong, J. K. Y.; Zerbetto, F.; Zhang, S. *J. Am. Chem. Soc.* **2002**, *124*, 2939.
(8) Zheng, X.; Sohlberg, K. *J. Phys. Chem. A* **2003**, *107*, 1207.
(9) Alteri, A.; Gatti, F. G.; Kay, E. R.; Leigh, D. A.; Martel, D.; Paolucci, F.; Slawin, A. M. Z.; Wong, J. K. Y. *J. Am. Chem. Soc.* **2003**, *125*, 8644.
(10) Grabuleda, X.; Ivanov, P.; Jaime, C. *J. Phys. Chem. B* **2003**, *107*, 7582.
(11) Pugh, C.; Bae, J.-Y.; Scott, J. R.; Wilkins, C. L. *Macromolecules* **1997**, *30*, 8139.
(12) Baschnagel, J.; Binder, K.; Doruker, P.; Gusev, A. A.; Hahn, O.; Kremer, K.; Mattice, W. L.; Müller-Plathe, F.; Murat, M.; Paul, W.; Santos, S.; Suter, U. W.; Tries, V. *Adv. Polym. Sci.* **2000**, *152*, 41.
(13) Helfer, C. A.; Xu, G.; Mattice, W. L.; Pugh, C. *Macromolecules* **2003**, *36*, 10071.
(14) Xu, G.; Rane, S. S.; Helfer, C. A.; Mattice, W. L.; Pugh, C. *Model. Simul. Mater. Sci. Eng.* **2004**, *12*, S59.
(15) Doruker, P.; Mattice, W. L. *Macromolecules* **1997**, *30*, 5520.
(16) Clancy, T. C.; Pütz, M.; Weinhold, J. D.; Curro, J. G.; Mattice, W. L. *Macromolecules* **2000**, *33*, 9452.
(17) Clancy, T. C.; Mattice, W. L. *Macromolecules* **2001**, *34*, 6482.
(18) Clancy, T. C.; Jang, J. H.; Dhinojwala, A.; Mattice, W. L. *J. Phys. Chem. B* **2001**, *105*, 11493.
(19) Raghunathan, G.; Jernigan, R. L. *Protein Sci.* **1997**, *6*, 2072.
(20) Abe, A.; Tasaki, K.; Mark, J. E. *Polym. J.* **1985**, *17*, 883.
(21) Cho, J.; Mattice, W. L. *Macromolecules* **1997**, *30*, 637.
(22) Metropolis, N.; Rosenbluth, A. W.; Rosenbluth, M. N.; Teller, A. H.; Teller, E. *J. Chem. Phys.* **1953**, *21*, 1087.
(23) Clancy, T. C.; Mattice, W. L. *J. Chem. Phys.* **2000**, *112*, 10049.
(24) Orwoll, R. A. In *Physical Properties of Polymers Handbook*; Mark, J. E., Ed.; American Institute of Physics: Woodbury, NY, 1996; p 82.

MA049159C